NJC

PAPER

View Article Online
View Journal

Cite this: DOI: 10.1039/c6nj01702a

Chemical transformation of ginsenoside Re by a heteropoly acid investigated using HPLC-MS^n/HRMS†

Yang Xiu,[a] Huanxi Zhao,[a] Yue Gao,[a] Wenlong Liu[a] and Shuying Liu*[ab]

Received (in Montpellier, France)
31st May 2016,
Accepted 18th August 2016

DOI: 10.1039/c6nj01702a

www.rsc.org/njc

The potential of heteropoly acid $H_3PW_{12}O_{40}$ to catalyze the chemical transformation of ginsenoside Re into rare ginsenosides was explored. This homogeneous catalyst can be recycled by extraction with diethyl ether. Eight resulting products were separated and identified through a developed high-performance liquid chromatography coupled with multistage tandem mass spectrometry and high-resolution mass spectrometry (HPLC-MS^n/HRMS) method. Multistage tandem mass spectrometry was employed to trace the source of fragments and determine fragmentation pathways. Also, high-resolution mass spectrometry was used for the accurate structural elucidation of fragments. Ginsenosides 25-OH-Rg_6 and 25-OH-F_4, consisting of the aglycone structures of "3β, 12β, 25-trihydroxy-dammar-20 (21/22)-ene", were obtained *via* chemical transformation for the first time. Chemical transformation pathways of ginsenoside Re were summarized, which involved deglycosylation, hydration, dehydration, and epimerization reactions. A carbenium ion mechanism was further employed to elucidate each transformation process, and the stability of carbenium ions was supposed to be responsible for the reaction pathways and selectivity.

Introduction

Ginseng, the root of *Panax ginseng* C. A. Mayer (Araliaceae), is one of the most valuable medicinal herbs in traditional Chinese medicine. It has been cultivated and taken as a medicinal resource in Asian countries for thousands of years.[1–3] Extensive modern research suggests that ginseng has wide pharmacological properties, such as immune system modulation, antistress, antihyperglycemic activities as well as potential cancer and aging process prevention.[4–8] Ginsenosides are the main active components responsible for the pharmaceutical activities and generally classified into three groups according to their genuine aglycone moieties, *i.e.* the ocotillol type, the oleanolic acid type and the dammarane type, which is subdivided into protopanaxadiol (PPD) and protopanaxatriol (PPT).[1,9] To date, more than 100 ginsenosides have been identified from ginseng and its processed products, most of which have demonstrated different pharmacological effects with respect to individual ginsenoside.[9–14] Many rare ginsenosides with significant pharmacological and biological effects are scarcely present or even absent in nature and can only be prepared through a transformation of major ginsenosides (Re, Rg_1, Rb_1, *etc.*). Therefore, methods including heating, acid or alkaline hydrolysis, and microbial and enzymatic transformation for the preparation of rare ginsenosides have attracted much attention recently.[15–26] For instance, Wang *et al.* investigated a total of 83 metabolites acquired from the transformation of ginsenosides from notoginseng by artificial gastric juice.[24] Vo *et al.* developed a kinetic model and simulated the heating process with kinetic parameters for the optimum production of ginsenoside Rg_3 by heat degradation of ginsenoside Rb_1.[25]

Among the conventional methods, the traditional use of homogeneous acid catalysts for ginsenoside chemical transformation exhibits high catalytic activity and low catalyst cost. Previously, we reported the studies of the hydrolysis of PPD and PPT-type ginsenosides by conventional homogeneous organic acids.[19,20] However, the large-scale use of acid suffers from catalyst recovery, unrecyclability, corrosion risk and treatment of the acid residue. Especially, the poor selectivity of the transformation of ginsenoside by acid catalysts strongly limits their application. Therefore, effective catalysts for the hydrolysis of ginsenosides are considerably in demand. Further studies are sill essential to identify the mechanisms and pathways of the chemical transformation of ginsenosides as well as those of the side reaction to improve the conversion, selectivity and yield of the main reaction.

Heteropoly acids (HPAs) are a unique type of solid acid consisting of early transition metal–oxygen anion clusters. They are recyclable and environmentally benign acid catalysts due to

[a] *Jilin Ginseng Academy, Changchun University of Chinese Medicine, Changchun 130117, P. R. China. E-mail: syliu@ciac.ac.cn*
[b] *Changchun Institute of Applied Chemistry, Chinese Academy of Sciences, Changchun, 130022, P. R. China*

† Electronic supplementary information (ESI) available. See DOI: 10.1039/c6nj01702a

their fascinating architectures and excellent physicochemical properties, such as strong Brønsted acidity, easy separation method, reusability, high proton mobility and regulable constituents. Among HPAs, the Keggin-type dodeca tungstophosphoric acid, *i.e.* $H_3PW_{12}O_{40}$, has been extensively researched and utilized in several industrial chemical processes.[27–32] Although the Keggin-type HPAs cannot be used as heterogeneous catalysts in polar solvent reactions, $H_3PW_{12}O_{40}$ could associate with diethyl ether molecules to form an ether-complex, which is insoluble in diethyl ether or in water and heavier than both of them. This ether-complex layer facilitates the extraction of $H_3PW_{12}O_{40}$ from aqueous reaction solution, retaining the reactant in the polar phase. After separation, the diethyl ether could be removed by evacuation, resulting in recovered $H_3PW_{12}O_{40}$ for reuse.[33,34] However, little attention has been devoted to the application of HPAs in chemical transformations of the active natural product, especially in the generation of rare ginsenosides.

High-performance liquid chromatography electrospray ionization mass spectrometry (HPLC-ESI-MS) has been proved to be a powerful tool for the separation and identification of ginsenosides.[19,20,35–40] Multistage tandem mass spectrometry (MS^n) analysis permits multiple isolation and fragmentation of precursor ions and allows the origins of the product ions to be unambiguously assigned. High-resolution mass spectrometry (HRMS) analysis provides more detailed and accurate information of molecular composition, which greatly facilitates the structural elucidation of the analytes and differentiation of isomers in combination with the collision induced dissociation (CID) technique.

Although studies on the chemical transformation of ginsenosides have been carried out, we herein applied HPAs as reusable catalysts to chemically transform ginsenoside Re. Eight newly generated ginsenosides are accurately identified *via* a HPLC-MS^n/HRMS method. The transformation pathways and mechanisms were further predicated and rationalized from a carbenium ion mechanism point of view. Notably, the aglycone structures of "3β, 12β, 25-trihydroxy-dammar-20 (21/22)-ene" were generated *via* the chemical transformation of PPT-type ginsenosides for the first time.

Experimental

Materials

All the ginsenoside authentic standards with over 98% purity were purchased from Beijing Wanjiashouhua Biological Technology Co., Ltd (Beijing, China). HPLC grade methanol and acetonitrile were acquired from Tedia (Fairfield, USA), whereas HPLC grade formic acid was acquired from Thermo Fisher (Waltham, USA). Heteropoly acid $H_3PW_{12}O_{40}{\cdot}nH_2O$ was bought from Sigma-Aldrich (St. Louis Missouri) and was calcinated at 300 °C to obtain $H_3PW_{12}O_{40}{\cdot}6H_2O$. Distilled water was purified using a Milli-Q water purification apparatus (Millipore, Bedford, USA).

HPLC-MS analysis

The high-performance liquid chromatography analysis was performed on a Dionex Ultimate 3000 system equipped with a quaternary bump, an autosampler and a thermostatically controlled column compartment. Analytes were separated by a Thermo Syncronis C_{18} column (100 mm × 2.1 mm i.d., 1.7 μm). The gradient solvent system consisted of solvent A (0.1% formic acid in water, v/v) and solvent B (acetonitrile), delivered at a flow rate of 0.2 mL min^{-1} and a temperature of 35 °C. The gradient elution was programmed as follows: 0–8 min (25–32% B); 8–10 min (32–35% B); 10–25 min (35–37% B); 25–28 min (37–40% B); 28–30 min (40–90% B) and 30–31 min (90% B). The injected sample volume was 5 μL.

High-resolution mass spectrometry was carried out on a Q Exactive hybrid quadrupole-orbitrap mass spectrometer (Thermo Scientific, San Jose, CA, USA), whereas multistage tandem mass spectra were acquired from an LTQ XL mass spectrometer (Thermo Scientific, San Jose, CA, USA). Both spectrometers were equipped with an electrospray ionization (ESI) source. Nitrogen was supplied as the sheath, auxiliary and sweep gas at flow rates of 35, 10 and 5 a.u., respectively. The capillary temperature was set at 320 °C. Ginsenosides were detected in the negative ion mode with a spray voltage of −4000 V. The capillary voltage was optimized to −32 V. Data were collected in centroid mode. CID experiments were performed on mass selected precursor ions using standard isolation and excitation procedures (an activation q value of 0.2 and an activation time of 30 ms). Ions were isolated using a width of m/z 1.0 (±0.5 m/z) and then subjected to the normalized collision energy. The scan range was from m/z 100 to 2000 for full scan mode and from m/z 260 to 1000 for CID experiments.

Procedure for the transformation of ginsenoside

The standard ginsenoside Re (1.01 mg) and catalyst $H_3PW_{12}O_{40}{\cdot}6H_2O$ (0.08 mmol) were accurately weighed and dissolved in 2 mL distilled water. The solution was introduced into a 5 mL glass vial under air, and then heated in a shaking bath at 80 °C for 2 h. Every 15 min, aliquots of solution were pipetted and diluted to a constant volume in an ice bath at 0 °C. The aqueous solution was extracted by diethyl ether in equal volume three times to separate the catalyst. The ether-complex layer was collected and evacuated to remove diethyl ether and to obtain $H_3PW_{12}O_{40}$ for reuse. To estimate the catalyst residue, the extracted solution that contained the residue of $H_3PW_{12}O_{40}$, unreacted ginsenoside Re and transformed products was further allowed to react for one more hour (denoted as 2 h-extracted sample). For comparison, the sample that reacted for 2 h was also prepared. As shown in Fig. S1 (ESI†), the TIC of the 2 h-extracted sample is similar to the TIC of the 1 h sample but significantly different from that of the 2 h sample, which indicates that most of the $H_3PW_{12}O_{40}$ has been removed. The recovery of $H_3PW_{12}O_{40}$ is calculated to be 98.2%. On the other hand, the aqueous layer was evaporated to dryness and dissolved in methanol (1 mL). Then the transformation solution was filtered through a 0.45 μm membrane before being subjected to HPLC-MS analysis.

Results and discussion

Determination of the molecular mass of ginsenoside by MS

All the compounds were identified through a comparison of the mass spectra and retention time with those of authentic

standards and empirical assignment of molecular structures through accurate mass of molecular ions, associated with multi-stage CID fragmentation. The identification of ginsenoside isomers was performed based on the characteristic chromatographic features of ginsenosides on the reverse-phase C18 column reported in the literature studies.

Ginsenoside molecules can be ionized through ESI in both positive and negative modes. The full-scan and CID mass spectra of the target ginsenosides were recorded in both modes. In positive ESI, a saponin molecule normally combines with an alkali metal ion, such as Na^+, a very common impurity that inevitably leaches from glassware. The gas-phase positive alkali metal ions have great binding affinity for the saccharide moiety of ginsenosides, and form fairly strongly bonded adducts. The internal energy of the resulting adduct molecules usually increases *via* this exothermic process, and being distributed over all internal degrees of freedom, which may facilitate the bond cleavages under CID conditions. As shown in Fig. S2 (ESI†), the MS^2 spectrum of the authentic standard of ginsenoside Re, in positive ESI mode, presents complex and irregular structural information on the cross-ring cleavage of saccharide but little direct information on aglycone and glycosidic cleavage. Correspondingly, in negative ESI, the neutral saponin molecules commonly lose one proton to form deprotonated molecular ions $[M–H]^-$, or associate loosely with one modifier ion to generate an adduct ion $[M + HCOO]^-$.[41] (Formic acid herein was employed as an organic modifier in the mobile phase to destroy the noncovalent interactions and to optimize the response of deprotonated analytes.) The formation of $[M–H]^-$ and $[M + HCOO]^-$ ions is endothermic and correlated with the acquisition of extra energy prior to fragmentation, which implies the lower internal energy of negative ions than that of their positive counterparts.[42] Therefore, data recorded in negative ion mode exhibited more clear spectra with much fewer fragments and were employed to obtain the straightforward structural information about ginsenosides in this study.

The molecular weight of Re was determined to be 946 Da, based on the $[M + HCOO]^-$ ion at *m/z* 991 and the $[M–H]^-$ ion at *m/z* 945. The MS^2 spectrum of the authentic standard of ginsenoside Re is shown in Fig. 1. The ions at *m/z* 179, 161 and 143 resulting from glycosidic bond cleavage confirmed the presence of hexose substitution (the ion at *m/z* 143 was derived from the rearrangement and removal of two H_2O molecules from the ion at *m/z* 179). Furthermore, the ions at *m/z* 131 and base peak *m/z* 101 represented two rearrangement ions after cross-ring cleavage at bonds 0 and 1 as well as at bonds 2 and 5 of the glucose residue, respectively.

MS^3 spectra on *m/z* 799, 783, 765, 637, 619 and 475 were carried out to trace the source of fragments. As shown in Fig. S3 (ESI†), the fragments were the same as those shown in Fig. 1. This is because in the negative ESI analysis of ginsenoside, MS^2 spectra could exhibit the deglycosylated fragment ions, which are the same as most of those in MS^n spectra, and provide sufficient information on saccharide substitutions in ginsenosides. Therefore, the fragmentation correlation was concluded to be: *m/z* 945 > *m/z* 799 > *m/z* 637 (619) > *m/z* 475 > *m/z* 391 and *m/z* 945 > *m/z* 783 > *m/z* 637 (619) > *m/z* 475 > *m/z* 391. Fragment ions at *m/z* 799 and 783 were 146 and 162 Da less than the $[M–H]^-$ ions at *m/z* 945, corresponding to the loss of one deoxyhexose and one hexose residue, respectively. Accordingly these two ions were assignable to $[M–Rha–H]^-$ (*m/z* 799) and $[M–Glc–H]^-$ (*m/z* 783) ions, which proved the presence of two different saccharide moieties with terminal rhamnose and glucose residues individually. Notably, the peak intensity of $[M–Glc–H]^-$ ions was distinctly higher than that of $[M–Rha–H]^-$ ions, suggesting that the glucose-terminated moiety was more reactive than the rhamnose-terminated one. The mass difference of 308 Da between the ions at *m/z* 945 and *m/z* 637 was in agreement with the total mass of one deoxyhexose and one hexose residue (146 Da + 162 Da), indicating the *m/z* 637 ion to be $[M–Glc–Rha–H]^-$. The ion at *m/z* 475, corresponding to the characteristic $[aglycone–H]^-$ ion of PPT, was generated through further loss of one glucose residue from the $[M–Glc–Rha–H]^-$ ion and is denoted as $[M–2Glc–Rha–H]^-$, indicating that there were totally one rhamnose and two glucose residues located at the saccharide substitutions. Two dehydration ions appeared at *m/z* 765 and 679, having a mass 18 Da lower than the ions at *m/z* 783 and 637, respectively. Since the dehydration ions could not be observed till the loss of one glucose residue from $[M–H]^-$ ions, in combination with the higher reactivity of the quaternary carbon at C-20 relative to the tertiary carbon at C-6 of the PPT aglycone, it is reasonable to assume that these two saccharide substitutions consisted of one glucose residue at C-20 and one glucose connected with one terminal rhamnose residue at C-6, respectively. The ion at *m/z* 205 originating from the cross-ring cleavage at bonds 0 and 2 on the glucose directly linked to aglycone provided further evidence for the number and connection of saccharide substitutions, as shown in the inset of Fig. 1.

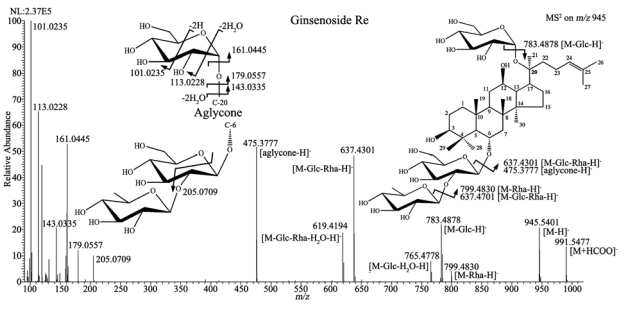

Fig. 1 High-resolution MS^2 spectrum from the $[M + HCOO]^-$ ion at *m/z* 991 and the fragmentation pathway of ginsenoside Re.

Structural characterization of the transformed ginsenoside by HPLC-MS^n/HRMS

Generally, ginsenosides could be transformed chemically by active H^+ in acidic solution through the hydrolysis of oligosaccharide moieties as well as dehydration, addition and cyclization reactions on the aglycone. Therefore, a certain amount of HPA was dissolved in deionized water, resulting in an acidic aqueous solution used for the transformation of ginsenoside Re at 80 °C for 1 h. The total ion chromatogram of the transformed products

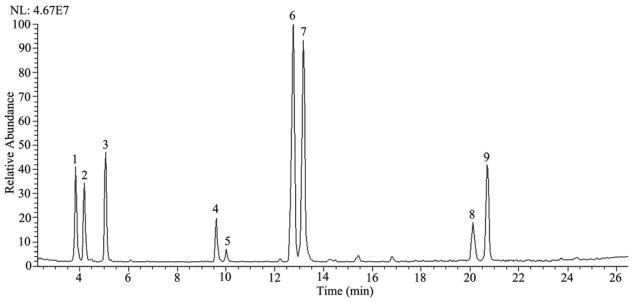

Fig. 2 Total ion chromatogram (TIC) of the products of ginsenoside Re chemical transformation by $H_3PW_{12}O_{40}$ at 80 °C for 1 h.

is shown in Fig. 2. Nine well-separated peaks were observed in the spectrum and denoted as compounds **1** to **9** in sequence. Compound **3** was unambiguously identified as the reactant Re through the comparison of the retention time and molecular mass with those of the authentic standard.

Compounds **4**, **5**, **6** and **7** were considered to be four isomers with the same molecular mass of 784 Da. Comparing to the authentic standard, 6 and 7 were assignable to ginsenosides 20(*S*)-Rg_2 and 20(*R*)-Rg_2, which were generated from the removal of the glucose residue at the C-20 position of Re and subsequent isomerization. Multistage tandem mass spectrometry and high-resolution mass spectrometry were performed for the structural elucidation of compound **4** as well as 20(*S*)-Rg_2 for comparison.

As shown in Fig. 3, the MS^3 fragmentation on the $[M–H]^-$ ions at *m*/*z* 783 provided one pair of differential ions at *m*/*z* 417 and 391 besides three pairs of identical ions at *m*/*z* 637, 619 and 475, which were corresponding to $[M–Rha–H]^-$, $[M–Rha–H_2O–H]^-$ and $[aglycone–H]^-$ ions. The differential ion pair at *m*/*z* 417 and 391 was further confirmed to be originating from the $[aglycone–H]^-$ ion of 4 and Rg_2 by the MS^4 spectra of the ion at *m*/*z* 475 (for the MS^n spectra of compound **5** and 20(*R*)-Rg_2, please see Fig. S4, ESI†). Furthermore, the accurate neutral loss between the differential ions and the $[aglycone–H]^-$ ion at *m*/*z* 475 was monitored by HRMS (Fig. S5, ESI†). For ginsenoside 20(*S*)-Rg_2, the neutral loss was 84.0936 Da, corresponding to C_6H_{12} with a mass error of 2.3 ppm, which was formed through bond cleavage between C-20 and C-21 with the residual charge retained on the aglycone, as illustrated in Fig. 3(b). On the other hand, compound **4** had a neutral loss of 58.0415 Da. The molecular mass of 58.0415 Da was determined as C_3H_6O with a mass error of 3.4 ppm, indicating the terminal tertiary alcohol structure bonding with two methyl groups, as shown in Fig. 3(d). Therefore, hydroxylation was determined to occur at the C-25 position of compounds **4** and **5**. And because of the same molecular mass of 4, 5 and Rg_2, it is reasonable to confirm the existence of unsaturated double bonds at C-20(21) or C-20(22), resulting from the dehydration of tertiary alcohol at the C-20 position. Consequently, compounds **4** and **5** could be structurally distinguished by the position of the double bond, which also led to their polarity differences. Since the Δ20(21) isomer tended to be more polar and eluted earlier from reversed-phase columns than its Δ20(22) counterparts, compounds **4** and **5** were concluded to be 25-OH-Rg_6 and 25-OH-F_4, which are rarely found in nature.[19,24,43,44]

Compounds **1** and **2** represented two Re-transformed ginsenosides with the $[M + HCOO]^-$ ion at *m*/*z* 847 and the $[M–H]^-$ ion at *m*/*z* 801, indicating a molecular mass of 802 Da (Fig. S6, ESI†). As shown in Fig. 4, the base peak at *m*/*z* 493 in the MS^2 spectrum on *m*/*z* 801 was 18 Da higher than the PPT aglycone ion at *m*/*z* 475, suggesting the hydration reaction on the unsaturated double bond at the C-24(25) position of the aglycone. Based on the regioselectivity of Markovnikov's rule for electrophilic addition to alkenes in acid solution, the hydroxyl group was apparently associated with C-25, resulting in the structure of 25-OH-PPT.[45] The neutral loss of 308 Da between the precursor $[M–H]^-$ ion at *m*/*z* 801 and the product ion at *m*/*z* 493 corresponded to the disaccharide moieties, one deoxyhexose and one hexose residue. In addition, the analogous chromatographic behaviours of these two peaks, such as the similar retention time and relative intensity as well as the identical patterns of the MS^2 spectrum, indicated the existence of C-20(*S*/*R*) epimers. The only difference

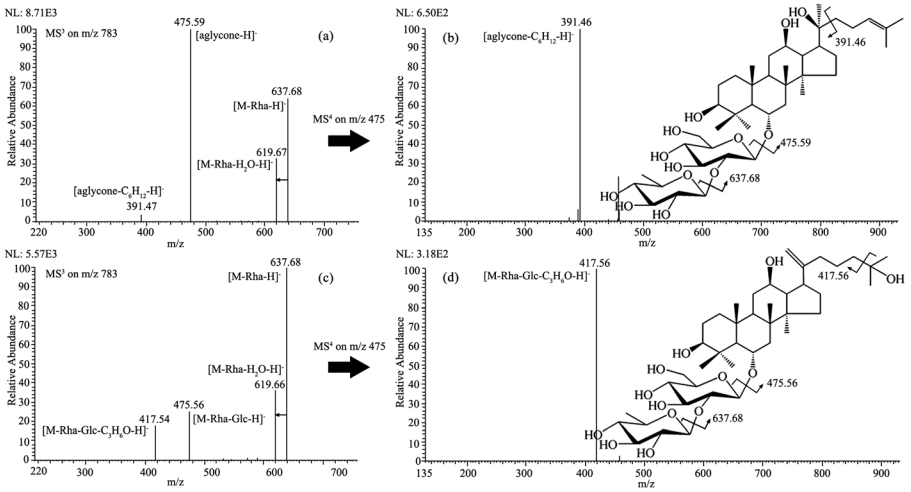

Fig. 3 MS^3 spectra of the ions at *m*/*z* 783 from the $[M + HCOO]^-$ ion of (a) ginsenoside 20(*S*)-Rg_2 and (c) 25-OH-Rg_6. Fragmentation pathways and MS^4 spectra of the ions at *m*/*z* 475 from the $[M + HCOO]^-$ ion of (b) ginsenoside 20(*S*)-Rg_2 and (d) 25-OH-Rg_6.

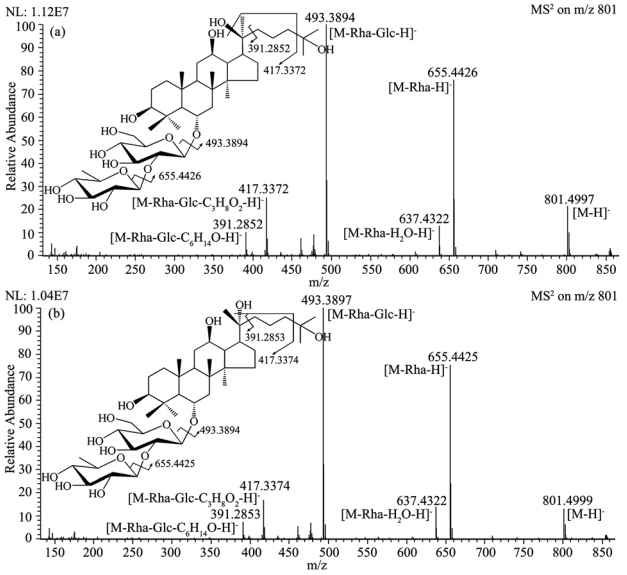

Fig. 4 High-resolution MS^2 spectra from the $[M-H]^-$ ion and the fragmentation pathways of ginsenoside (a) 20(*S*)-Rf_2 and (b) 20(*R*)-Rf_2.

between the epimers was the configuration of the chiral carbon at C-20. Because the 20(*S*)-epimer eluted earlier than the correlative 20(*R*)-epimer, compounds **1** and **2** were identified as ginsenoside 20(*S*)-Rf_2 and 20(*R*)-Rf_2, respectively.[20,44] Moreover, ginsenoside 25-OH-PPT is expected to represent safe and effective therapeutic agents, since its 25-OH-PPD counterpart has already exhibited potent anticancer activity.[46]

Similarly, structural elucidation for the isomers of compounds **8** and **9** with a molecular mass of 766 Da was performed (Fig. 5 and Fig. S7, ESI†). Owing to the same neutral loss and fragmentation patterns of the precursor ions at *m*/*z* 765 in Fig. 5 and *m*/*z* 801 in

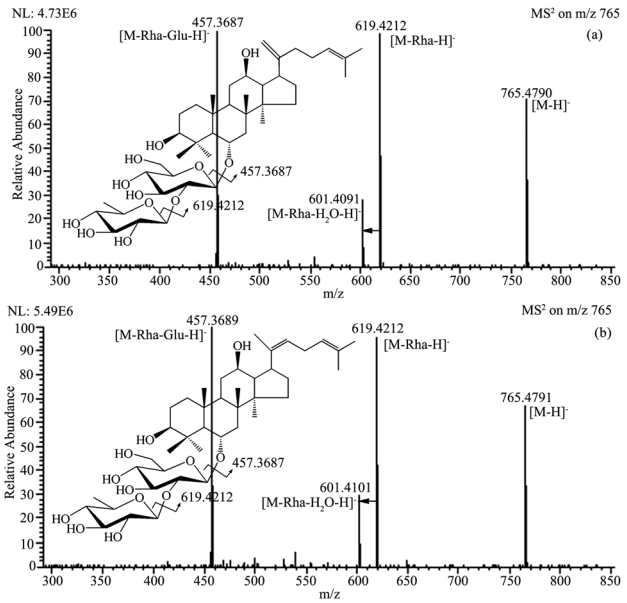

Fig. 5 High-resolution MS^2 spectra from the $[M-H]^-$ ion and the fragmentation pathways of ginsenoside (a) Rg_6 and (b) F_4.

Fig. 4, the saccharide moiety of 8 and 9 was considered to be identical to that of ginsenoside Rf_2. Comparing to the PPT aglycone ion at *m*/*z* 475, the ion at *m*/*z* 457 with −18 Da mass difference indicated the occurrence of dehydration reaction. The deglycosylation of the glucose moiety at C-20 generated a tertiary alcohol group, which was responsible for the dehydration. Therefore, a new double bond was expected to be located at C-20(21) or C-20(22) on the aglycone, resulting in two Re-transformed ginsenoside isomers. Consequently, it is concluded that compounds **8** and **9** originated from Re through deglycosylation followed by dehydration at the C-20 position and were assigned as ginsenoside Rg_6 and F_4, respectively. It is worth noting that, under the same CID conditions, there was no fragment further generated from the aglycone ions at *m*/*z* 457, since these two double bonds led to a relatively stable rigid aglycone. The spectral information on all the transformed products is summarized in Table 1.

Generally, the ionized ginsenoside molecules usually lose saccharide substitutions in sequence to generate an aglycone moiety in CID experiment in negative ESI mode. Through the observed neutral loss, the number and connection of saccharide substitutions as well as the structural difference to PPT aglycone could be directly identified. And the aglycone moiety could be further fragmented to generate specific ions used for structural discrimination. In this study, the aglycone moieties of all the 8 transformed compounds can be classified into four types, *i.e.* (a) 3β, 12β, 20-trihydroxy-dammar-24-ene (Re and 20(*S*/*R*)-Rg_2); (b) 3β, 12β-dihydroxy-dammar-20(21/22), 24-diene (Rg_6 and F_4); (c) 3β, 12β, 20, 25- tetrahydroxy-dammarane (20(*S*/*R*)-Rf_2); and (d) 3β, 12β, 25-trihydroxy-dammar-20 (21/22)-ene (25-OH-Rg_6 and 25-OH-Rg_4). All the aglycone moieties exhibited absolutely different fragmentation pathways. In CID experiments, aglycone (a) produced ions at *m*/*z* 475 and 391. The ion at *m*/*z* 475 is the typical deprotonated ion of PPT aglycone, whereas *m*/*z* 391 resulted from the bond cleavage between C-20 and 22 with 84 Da neutral loss. Only one ion at *m*/*z* 457, 18 Da lower than PPT aglycone, was obtained from aglycone (b). This is due to the rigid framework derived from the dehydration at C-20 of PPT and hence difficulty in dissociation. Aglycone (c) produced three ions at *m*/*z* 491, 417 and 391, which correspond to the hydrated ion of PPT aglycone, the ion with bond cleavage at C-24(25) and following dehydration of one water molecule, and the ion with bond cleavage at C-20(22). For aglycone (d), which is the isomer of aglycone (a), the fragmentation of *m*/*z* 417 is conducive to the isomer differentiation. This ion is considered to have resulted from the bond cleavage between C-24 and 25, with a neutral loss of 58 Da. Furthermore, based on the developed HPLC-MS^n/HRMS method, precise molecular weight information could be obtained, which was useful for the accurate structural elucidation of fragments, and the origins of fragments were recognized, which was the foundation of structure analysis. The combined use of HRMS and MS^n analyses provides reliable results of structural elucidation for unknown ginsenosides.

Pathways and mechanisms of the chemical transformation of Re in acid solution

In summary, a total of eight ginsenosides, 20(*S*/*R*)-Rf_2, 20(*S*/*R*)-Rg_2, 25-OH-Rg_6/F_4, Rg_6 and F_4, are available from the chemical

Table 1 Major ions (*m*/*z*) observed in the HRMS spectra of the chemical transformation products of ginsenoside Re

Peak	Identification	Measured mass (*m*/*z*)	Molecular formula $[M-H]^-$	Theoretical mass	Mass error (ppm)	MS^2 fragment ions
1	20(*S*)-Rf_2	801.4997	$C_{42}H_{73}O_{14}$	801.5000	−0.4	847.5044 $[M + HCOO]^-$, 655.4426 $[M–Rha–H]^-$, 637.4322 $[M–Rha–H_2O–H]^-$, 493.3894 $[M–Rha–Glc–H]^-$, 417.3372 $[M–Rha–Glc–C_3H_8O_2–H]^-$, 391.2852 $[M–Rha–Glc–C_6H_{14}O–H]^-$
2	20(*R*)-Rf_2	801.4999	$C_{42}H_{73}O_{14}$	801.5000	−0.4	847.5044 $[M + HCOO]^-$, 655.4425 $[M–Rha–H]^-$, 637.4322 $[M–Rha–H_2O–H]^-$, 493.3897 $[M–Rha–Glc–H]^-$, 417.3374 $[M–Rha–Glc–C_3H_8O_2–H]^-$, 391.2853 $[M–Rha–Glc–C_6H_{14}O–H]^-$
3	Re	945.5401	$C_{48}H_{81}O_{18}$	945.5423	−2.3	991.5477 $[M + HCOO]^-$, 799.4830 $[M–Rha–H]^-$, 783.4878 $[M–Glc–H]^-$, 765.4778 $[M–Glc–H_2O–H]^-$, 637.4301 $[M–Glc–Rha–H]^-$, 619.4194 $[M–Glc–Rha–H_2O–H]^-$, 475.3777 $[aglycone–H]^-$
4	25-OH-Rg_6	783.4885	$C_{42}H_{71}O_{13}$	783.4895	−1.2	637.4314 $[M–Rha–H]^-$, 619.4203 $[M–Rha–H_2O–H]^-$, 475.3781 $[M–Rha–Glc–H]^-$, 417.3361 $[M–Rha–Glc–C_3H_6O–H]^-$
5	25-OH-F_4	783.4887	$C_{42}H_{71}O_{13}$	783.4895	−1.0	637.4315 $[M–Rha–H]^-$, 619.4207 $[M–Rha–H_2O–H]^-$, 475.3785 $[M–Rha–Glc–H]^-$, 417.3367 $[M–Rha–Glc–C_3H_6O–H]^-$
6	20(*S*)-Rg_2	783.4879	$C_{42}H_{71}O_{13}$	783.4895	−2.0	637.4308 $[M–Rha–H]^-$, 619.4198 $[M–Rha–H_2O–H]^-$, 475.3780 $[aglycone–H]^-$, 391.2844 $[aglycone–C_6H_{12}–H]^-$
7	20(*R*)-Rg_2	783.4881	$C_{42}H_{71}O_{13}$	783.4895	−1.8	637.4308 $[M–Rha–H]^-$, 619.4197 $[M–Rha–H_2O–H]^-$, 475.3780 $[aglycone–H]^-$, 391.2845 $[aglycone–C_6H_{12}–H]^-$
8	Rg_6	765.4790	$C_{42}H_{69}O_{12}$	765.4789	0.1	619.4212 $[M–Rha–H]^-$, 601.4091 $[M–Rha–H_2O–H]^-$, 457.3687 $[M–Rha–Glu–H]^-$
9	F_4	765.4791	$C_{42}H_{69}O_{12}$	765.4789	0.3	619.4212 $[M–Rha–H]^-$, 601.4101 $[M–Rha–H_2O–H]^-$, 457.3689 $[M–Rha–Glu–H]^-$

transformation of Re in the $H_3PW_{12}O_{40}$ dissolved strongly acidic aqueous phase. Therefore, the observed transformation pathways involve deglycosylation at the C-20 position prior to hydration, dehydration and epimerization reaction occurring on the side chain, as demonstrated in Scheme 1.

Deglycosylation of Re primarily occurred to yield the main products of ginsenoside 20(*S*/*R*)-Rg_2 through the hydrolysis of the saccharide moiety at C-20 rather than the one at C-6. This can be rationalized by the carbenium ion mechanism: the cleavage of the glycosidic bond at C-20 tends to generate the tertiary carbenium ion with more stability on the chiral carbon atom in a much lower activation energy pathway compared to the formation of the secondary carbenium ion at C-6 on the rigid backbone. Therefore, the deglycosylation reactivity of C-20 is distinctly higher than that of C-6, leading to the preferential hydrolysis of the saccharide moiety and hence the formation of 20(*S*/*R*)-Rg_2 with tertiary alcohol at the C-20 position. Intriguingly, the generated epimers, 20(*S*)-Rg_2 and 20(*R*)-Rg_2, are present in almost equal amounts. This is due to the trigonal planar molecular geometry of the sp^2 hybridized carbenium intermediate, which allows the nucleophilic attack in two non-selective avenues on either side of the plane, yielding a mix of epimers in equal proportion, as illustrated in Fig. 6.[47]

After deglycosylation at the C-20 position, the active tertiary alcohol could be further eliminated in the acidic aqueous phase through an E1 mechanism, resulting in ginsenosides Rg_6 and F_4. As shown in Scheme 2, the protonation of the alcoholic oxygen firstly generates an oxonium ion, providing a leaving group of a neutral water molecule, which is ideal to start the elimination reaction. The loss of the leaving group generates a carbenium intermediate followed by the removal of the hydrogen from the β-carbon to result in the creation of the double bond at C20(21) and C20(22). The generation of carbenium is the rate-determining step and related to the stability of the carbenium intermediate. Therefore, the tertiary hydroxyl at C-20 showed higher reactivity in the dehydration reaction than those at C-3 and C-12 which bear the secondary carbenium ion. Moreover, the content ratio of Rg_6/F_4 is equal to 3 : 7 in accordance with Zaitsev's rule which predicts that the most substituted alkene will be typically stable and favoured in elimination reactions.[48,49]

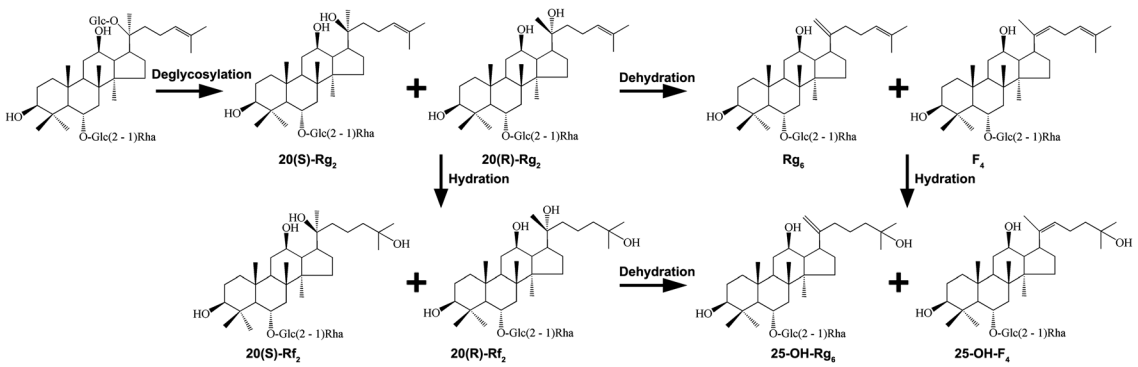

Scheme 1 Chemical transformation pathway of ginsenosides Re catalyzed by $H_3PW_{12}O_{40}$. Glc, β-D-glucopyranosyl; Rha, α-L-rhamnopyranosyl.

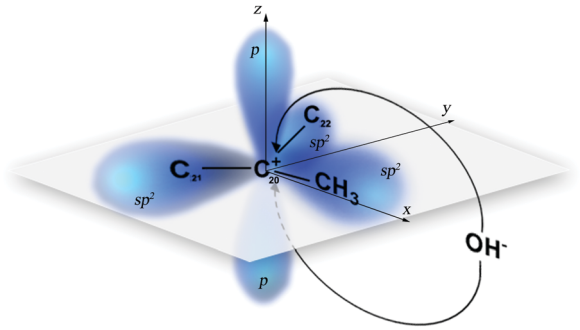

Fig. 6 Representation of the epimerization of C-20 resulting from the non-selective attack of the hydroxyl group on the trigonal planar sp^2 hybridized carbon.

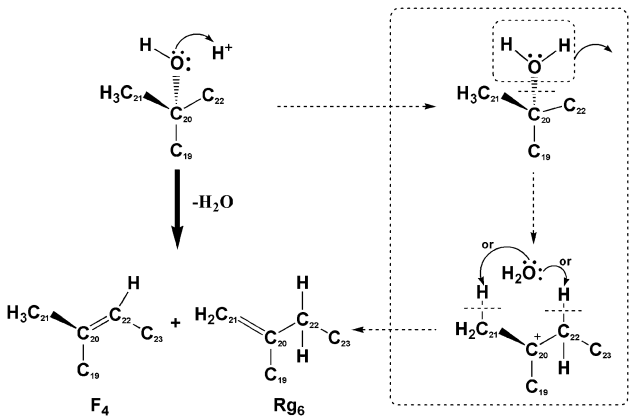

Scheme 2 The proposed carbenium ionic route of dehydration of ginsenoside Rg_2.

The stability of the carbenium ion also plays a decisive role in the hydration on the double bond at C-24(25) to yield 20(*S*/*R*)-Rf_2 and 25-OH-Rg_6/F_4. As shown in Scheme 3, the electrophilic attack of hydrogen cations gives rise to the break of the double bond, protonation of C-24 and creation of a positive charge on C-25,

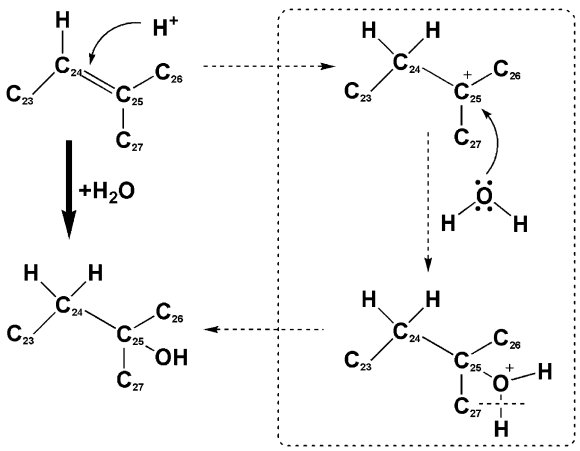

Scheme 3 The proposed carbenium ionic route of hydration on the double bond between C-24 and C-25.

forming a tetravalent tertiary carbenium intermediate. This is the rate-determining step. The more stable the carbenium intermediate is, the easier it is to form. Afterwards, the lone-pair electrons of water molecules further attack on the carbenium ion to hydroxylate by leaving the catalytic hydrogen cations, resulting in the hydrated products. This reaction pathway is thermodynamically favoured compared to the hydroxylation on the C-24 atom, which undergoes the generation of a secondary carbenium ion with less stability and higher activation energy.[50,51]

Since there is chemical equilibrium between alcohols and alkenes in acid environments, both of the hydrations on the double bond at C-24(25) atoms and the dehydration on C-20(21/22) atoms of PPT type ginsenosides are considered to be reversible reactions, which could be rationalized from the carbenium ion mechanism point of view. Therefore, the shift of both reversible transformation pathways depends on the reaction temperature and catalytic activity. In our previous studies on the chemical transformation of PPT and PPD type ginsenosides using a volatile organic acid, such as formic acid and acetic acid, no aglycone structures of 3β, 12β, 25-trihydroxy-dammar-20 (21/22)-ene are observed.[19,20] In the present study, 25-OH-Rg_6/F_4 could be produced through further dehydration of 20(*R*/*S*)-Rf_2 or hydration of Rg_6/F_4. This is attributed to the strong acidity of HPA in aqueous solutions which promote the loss of the leaving group and are conductive to the formation of stable carbenium ions at C-20 and C-25 of the aglycone to obtain dynamic equilibrium of those generated ginsenosides in the transformation process.

Conclusions

The heteropoly acid $H_3PW_{12}O_{40}$ was developed for the chemical transformation of ginsenoside Re and recycled through simple extraction by diethyl ether. Eight products were obtained and identified based on a HPLC-MS^n/HRMS method. Particularly, four isomeric products of 784 Da could be easily identified through the developed method. The transformation pathway involves the acid-catalyzed deglycosylation, hydration, dehydration and isomerization reactions, all of which proceed through the carbenium ion mechanism. 25-OH-Rg_6 and 25-OH-F_4, consisting of the aglycone structures of "3β, 12β, 25-trihydroxy-dammar-20 (21/22)-ene", were generated *via* chemical transformation for the first time, which provides a prospective feasibility to transform certain effective and rare ginsenosides. Although there is still a need to improve the selectivity of the transformation reaction, which is precisely what we are focusing on, HPA catalysts open up a clean, economical and environmentally benign process in the chemical transformation of active natural products.

Acknowledgements

This work was financially supported by the Science and Technology Development Plan Project of Jilin Province (20160520123JH) and Special Fund for Agro scientific Research in the Public Interest (201303111).

Notes and references

1 D. H. Kim, *J. Ginseng Res.*, 2012, **36**, 1–15.
2 L. Jia, Y. Zhao and X. J. Liang, *Curr. Med. Chem.*, 2009, **16**, 2924–2942.
3 Y. Z. Xiang, H. C. Shang, X. M. Gao and B. L. Zhang, *Phytother. Res.*, 2008, **22**, 851–858.
4 A. S. Attele, J. A. Wu and C. S. Yuan, *Biochem. Pharmacol.*, 1999, **58**, 1685–1693.
5 M. S. Lee, E. J. Yang, J. I. Kim and E. Ernst, *J. Alzheimers Dis.*, 2009, **18**, 339–344.
6 J. M. Lü, Q. Yao and C. Chen, *Curr. Vasc. Pharmacol.*, 2009, **7**, 293–302.
7 H. J. Kim, P. Kim and C. Y. Shin, *J. Ginseng Res.*, 2013, **37**, 8–29.
8 J. Y. Park, P. Choi, H. K. Kim, K. S. Kang and J. Ham, *J. Ginseng Res.*, 2016, **40**, 62–67.
9 L. P. Christensen, *Adv. Food Nutr. Res.*, 2009, **55**, 1–99.
10 S. F. Nabavi, A. Sureda, S. Habtemariam and S. M. Nabavi, *J. Ginseng Res.*, 2015, **39**, 299–303.
11 S. J. Lee, W. J. Lee, S. E. Chang and G. Y. Lee, *J. Ginseng Res.*, 2015, **39**, 238–242.
12 G. C. Han, S. K. Ko, J. H. Sung and S. H. Chung, *J. Agric. Food Chem.*, 2007, **55**, 10641–10648.
13 Y. Usami, Y. N. Liu, A. S. Lin, M. Shibano, T. Akiyama, H. Itokawa, S. L. Morris-Natschke, K. Bastow, R. Kasai and K. H. Lee, *J. Nat. Prod.*, 2008, **71**, 478–481.
14 J. S. Jung, J. A. Shin, E. M. Park, J. E. Lee, Y. S. Kang, S. W. Min, D. H. Kim, J. W. Hyun, C. Y. Shin and H. S. Kim, *J. Neurochem.*, 2010, **115**, 1668–1680.
15 B. H. Han, M. H. Park, Y. N. Han, L. K. Woo, U. Sankawa, S. Yahara and O. Tanaka, *Planta Med.*, 1982, **44**, 146–149.
16 P. Pietta, P. Mauri and A. Rava, *J. Chromatogr.*, 1986, **362**, 291–297.
17 I. H. Park, N. Y. Kim, S. B. Han, J. M. Kim, S. W. Kwon, H. J. Kim, M. K. Park and J. H. Park, *Arch. Pharmacal Res.*, 2002, **25**, 428–432.
18 E. A. Bae, M. J. Han, E. J. Kim and D. H. Kim, *Arch. Pharmacal Res.*, 2004, **27**, 61–67.
19 X. Zhang, F. Song, M. Cui, Z. Liu and S. Liu, *Planta Med.*, 2007, **73**, 1225–1229.
20 W. Wu, Q. J. Qin, Y. Y. Guo, J. H. Sun and S. Y. Liu, *J. Agric. Food Chem.*, 2012, **60**, 10007–10014.
21 D. Wang, P. Y. Liao, H. T. Zhu, K. K. Chen, M. Xu, Y. J. Zhang and C. R. Yang, *Food Chem.*, 2012, **132**, 1808–1813.
22 N. Yamabe, K. I. Song, W. Lee, I. H. Han, J. H. Lee, J. Ham, S. N. Kim, J. H. Park and K. S. Kang, *J. Ginseng Res.*, 2012, **36**, 256–262.
23 J. Y. Wan, P. Liu, H. Y. Wang, L. W. Qi, C. Z. Wang, P. Li and C. S. Yuan, *J. Chromatogr. A*, 2013, **1286**, 83–92.
24 J. R. Wang, L. F. Yau, R. Zhang, Y. Xia, J. Ma, H. M. Ho, P. Hu, M. Hu, L. Liu and Z. H. Jiang, *J. Agric. Food Chem.*, 2014, **62**, 2558–2573.
25 H. T. Vo, J. Y. Cho, Y. E. Choi, Y. S. Choi and Y. H. Jeong, *J. Ginseng Res.*, 2015, **39**, 304–313.
26 Y. Yuan, Y. B. Hu, C. X. Hu, J. Y. Leng, H. L. Chen, X. S. Zhao, J. Gao and Y. F. Zhou, *J. Mol. Catal. B: Enzym.*, 2015, **120**, 60–67.
27 I. V. Kozhevnikov, *Chem. Rev.*, 1998, **98**, 171–198.
28 I. V. Kozhevnikov, *J. Mol. Catal. A: Chem.*, 2007, **262**, 86–92.
29 I. V. Kozhevnikov, *J. Mol. Catal. A: Chem.*, 2009, **305**, 104–111.
30 N. Mizuno, K. Yamaguchi and K. Kamata, *Coord. Chem. Rev.*, 2005, **249**, 1944–1956.
31 Y. B. Huang and Y. Fu, *Green Chem.*, 2013, **15**, 1095–1111.
32 W. Deng, Q. Zhang and Y. Wang, *Dalton Trans.*, 2012, **41**, 9817–9831.
33 H. Wu, *J. Biol. Chem.*, 1920, **43**, 189–220.
34 J. Tian, J. Wang, S. Zhao, C. Jiang, X. Zhang and X. Wang, *Cellulose*, 2010, **17**, 587–594.
35 S. Li, S. Lai, J. Song, C. Qiao, X. Liu, Y. Zhou, H. Cai, B. Cai and H. Xu, *J. Pharm. Biomed. Anal.*, 2010, **53**, 946–957.
36 N. Fuzzati, B. Gabetta, K. Jayakar, R. Pace and F. Peterlongo, *J. Chromatogr. A*, 1999, **854**, 69–79.
37 M. Cui, F. Song, Y. Zhou, Z. Liu and S. Liu, *Rapid Commun. Mass Spectrom.*, 2000, **14**, 1280–1286.
38 F. Song, Z. Liu, S. Liu and Z. Cai, *Anal. Chim. Acta*, 2005, **531**, 69–77.
39 S. Liu, M. Cui, Z. Liu and F. Song, *J. Am. Soc. Mass Spectrom.*, 2004, **15**, 133–141.
40 F. Wu, H. Sun, W. Wei, Y. Han, P. Wang, T. Dong, G. Yan and X. Wang, *J. Sep. Sci.*, 2011, **34**, 3194–3199.
41 Z. Wu, W. Gao, M. A. Phelps, D. Wu, D. D. Miller and J. T. Dalton, *Anal. Chem.*, 2004, **76**, 839–847.
42 R. B. Cole, *Electrospray and MALDI Mass Spectrometry*, Wiley John & Sons, 2010.
43 S. W. Kwon, S. B. Han, I. H. Park, J. M. Kim, M. K. Park and J. H. Park, *J. Chromatogr. A*, 2001, **921**, 335–339.
44 H. Yang, Y. D. Lee, K. B. Kang, J. Y. Kim, S. O. Kim, Y. H. Yoo and S. H. Sung, *J. Pharm. Biomed. Anal.*, 2015, **109**, 91–104.
45 S. Liu, C. Rong and T. Lu, *J. Phys. Chem. A*, 2014, **118**, 3698–3704.
46 W. Wang, E. R. Rayburn, Y. Zhao, H. Wang and R. Zhang, *Cancer Lett.*, 2009, **278**, 241–248.
47 Q. Xiang, Y. Y. Lee, P. O. Petterson and R. Torget, *Appl. Biochem. Biotechnol.*, 2003, **105**, 505–514.
48 C. M. Rosado-Reyes, W. Tsang, I. M. Alecu, S. S. Merchant and W. H. Green, *J. Chromatogr. A*, 2013, **117**, 6724–6736.
49 M. M. Toteva and J. P. Richard, *J. Am. Chem. Soc.*, 1996, **118**, 11434–11445.
50 P. K. Chattaraj, U. Sarkar and D. R. Roy, *Chem. Rev.*, 2006, **106**, 2065–2091.
51 A. Aizman, R. Contreras, M. Galván, A. Cedillo, J. C. Santos and E. Chamorro, *J. Phys. Chem. A*, 2002, **106**, 7844–7849.

